Radiation Physics and Chemistry 232 (2025) 112701

Contents lists available at ScienceDirect

Radiation Physics and Chemistry

journal homepage: www.elsevier.com/locate/radphyschem

Performance evaluation of a new dosimetric system for lens dosimetry made using 3D printing

G.G. Nascimento [a,*], O. Rodrigues Jr [a], M. Savi [b], D. Villani [a,c], M.P.A. Potiens [a]

[a] Centro de Metrologia das Radiações Ionizantes – Instituto de Pesquisas Energéticas e Nucleares (USP/SP), Brazil
[b] Departamento Acadêmico de Saúde - Instituto Federal de Santa Catarina (IFSC/SC), Brazil
[c] Deutsches Elektronen-Synchrotron - (DESY/ZN), Brazil

ARTICLE INFO

Handling Editor: Dr. Chris Chantler

Keywords:
Dosimeter holder
Dosimetry lens
LiF:Mg,Ti
Printing 3D

ABSTRACT

For some years now, the radiation dose received by the lens of the eye has been the subject of discussion in the field of radiological protection. As a result, dose limits have been reduced, and the lens has come to be considered a critical organ. This concern has become more intense in the interventional radiology environment, where occupational exposure is significant, increasing the likelihood of developing cataracts caused by radiation. The present study aims to evaluate the performance of a new model of dosimeter holder, manufactured by means of 3D printing, designed for lens dosimetry, comparing its performance using a cylinder phantom recommended by ICRU and an anthropomorphic simulator developed by 3D printing.

1. Introduction

A few years ago, the dose of radiation received by the lens of the eye became an important topic in discussions related to radiological protection (Behrens, 2011). This growing concern resulted in a review of existing guidelines and, consequently, a reduction in the recommendations regarding permitted dose limits. As a result of this process, the lens of the eye was formally included in the category of critical organs, highlighting the importance of considering its protection appropriately in the context of radiation exposure (ICRP, 2007).

During interventional radiology procedures, professionals involved in this area are frequently exposed to ionizing radiation, which poses a significant risk of compromising eye health, especially in the lens region. Therefore, monitoring body areas subject to this exposure is essential to mitigate the risks associated with ionizing radiation (Barbosa et al., 2019).

Radiation-induced cataracts (from exposure to ionizing radiation) are a significant concern for occupationally exposed individuals (OEI). Prolonged exposure of the lens of the eye to ionizing radiation can cause changes in the crystals of the lens of the eye, resulting in detectable opacity or the development of cataracts (ICRP, 2012). Cataracts occur as a result of the accumulation of damaged or dead cells within the lens of the eye that are not naturally removed. In interventional radiology procedures, operators are frequently exposed to X-rays. However, some studies evaluating interventional cardiologists indicate an increased prevalence of cataracts in this specific occupation (Bitarafan Rajabi et al., 2015).

The dose to the lens of the eye is not measurable and is therefore usually assessed by measuring the personal dose equivalent, Hp(d), where d is the depth of the region of interest. To monitor the ocular lens dose, a specific depth of 3 mm has been implemented by the International Commission on Radiological Units and Measurements (ICRU) and recommended by the International Commission on Radiological Protection (ICRP) (ICRU, 2017; ICRP, 1991).

For individual monitoring, the personal dose equivalent, Hp(d), is used. Hp(d) is the soft tissue dose equivalent at an appropriate depth, d, below a specific point on the body. The specific point is usually given by the position where the dosimeter is positioned. Recommended values for d are chosen for the evaluation of several doses: $d = 10$ mm for effective dose, $d = 0.07$ mm for dose to the skin and extremities of the hands and feet, and $d = 3$ for dose to the lens of the eye (Petoussi-Henss et al., 2020). However, in many countries, the quantity Hp(3) has never been implemented in legal metrology and only the quantities Hp(0.07) and Hp(10) are used to monitor the radiation exposure of workers.

In this work, a dosimeter holder for lens dosimetry was developed using 3D printing techniques. The dosimeter holders were positioned in

This article is part of a special issue entitled: ISRP-16 published in Radiation Physics and Chemistry.

* Corresponding author.
E-mail address: gabrielgn@alumni.usp.br (G.G. Nascimento).

https://doi.org/10.1016/j.radphyschem.2025.112701
Received 30 December 2024; Received in revised form 10 March 2025; Accepted 11 March 2025
Available online 12 March 2025

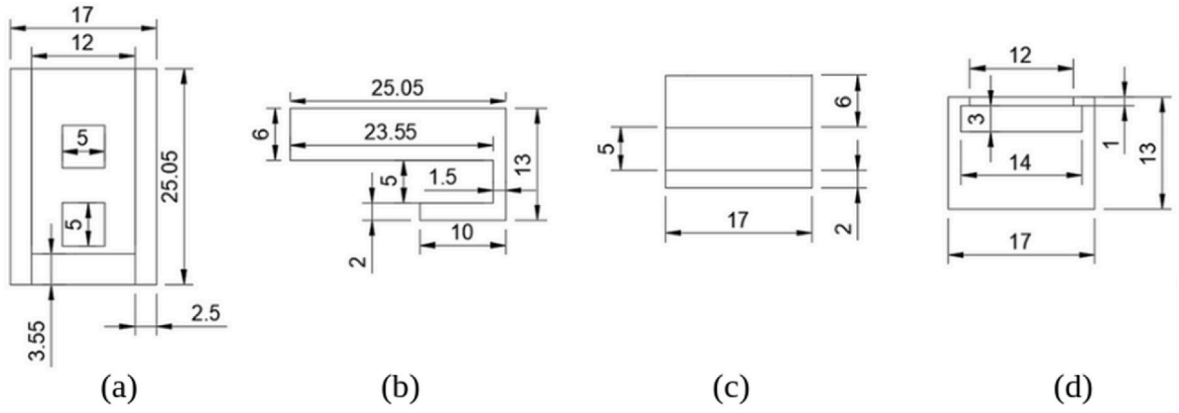

Fig. 1. Views of the dosimeter holder on the fusion: (a) Upper view, (b) Side view, (c) Back view and (d) Front view.

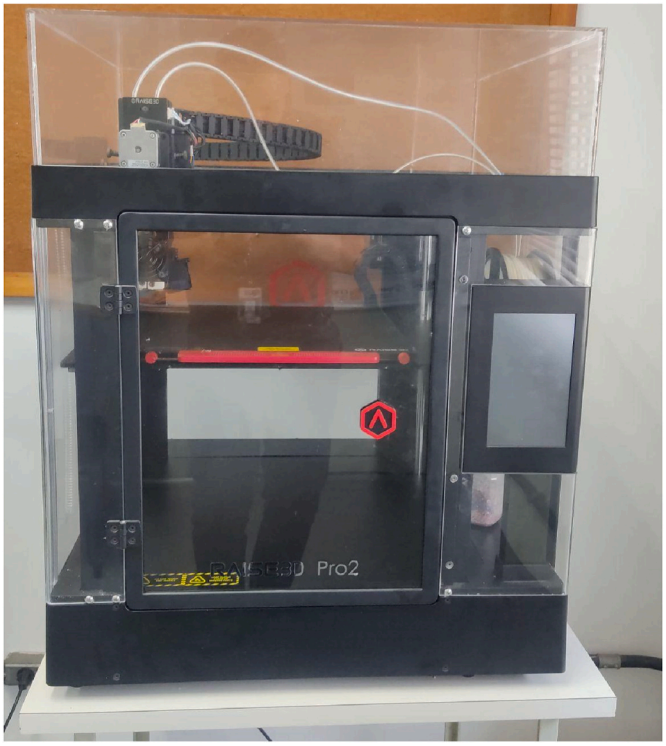

Fig. 2. Raise Pro2 3D printer.

Table 1
Print settings.

Heated Bed Temperature	Extruder Temperature	Printing Speed	Infill Density	Infill Speed
60 °C	190 °C	50.00 mm/s	15 %	80.00 mm/s

two phantom models, the first model consists of the standard cylinder recommended by ICRU, the second model is an anthropomorphic phantom developed using 3D printing (ICRU, 1985; Savi, 2022).

In the literature, it is possible to find other dosimeter holders for eyes, such as the model for stereotactic radiosurgery (Alyahyawi et al., 2019) and the model for interventional radiology (Surić Mihić et al., 2020). However, generally, the main choice of the authors for this type of prototype is the filament based on Acrylonitrile Butadiene Styrene (ABS). In this work, the thermoplastic filament based on Polylactic Acid (PLA) is used.

The International Organization for Standardization (ISO), in its publication 12,794, establishes some conditions for a dosimeter to be used in lens dosimetry (ISO 12794, 2014). ISO 12794 recommends that irradiations be performed at 0°, 20°, 40° and 60° in relation to the radiation beam; however, in this study, angles of 0° and 90° in relation to the radiation beam were used.

2. Materials and methods

2.1. 3D printing parameters

The dosimeter holder was created using the free version of the 3D modeling software Fusion 360, developed by Autodesk. The software allows parametric 3D modeling, simulation and analysis, among other available tools. The measurements used to develop this dosimeter holder (in mm) can be seen in Fig. 1.

The prints were made using a Pro2 3D printer (Fig. 2), sold by Raise 3D. This printer uses Fused Filament Fabrication (FFF) technology. This technology is widely popular and widely used in the market.

In the FFF technique, the filament is extruded and melted in a thin layer. After this preheating, the filament passes through a heated nozzle that aligns and deposits the melted filament in successive layers, which soon solidify, forming the final piece.

It used a thermoplastic filament commercially known as polylactic acid (PLA), with a diameter of 1.75 mm. Some of the main print settings can be observed in Table 1:

It is important to consider that printing parameters may vary depending on the specific characteristics of the filament, such as color, brand, and storage time after opening. This may require adjustments to the 3D printer parameters.

The dosimeter holder was developed for use on the temples of glasses, with the printing design being modifiable to better suit the specifications of each pair of glasses. The dosimeter holder features a design capable of accommodating up to 2 chip-shaped detectors, in addition to having a type of drawer for protecting and fixing the detectors (Fig. 3).

2.2. Thermoluminescent dosimeter

Thirty thermoluminescent dosimeters (TLDs) of Lithium Fluoride doped with Magnesium and Titanium (LiF:Mg,Ti) in the form of chips, with dimensions of 3.2× 3.2 × 0.89 mm, commercially known as TLD-100, were selected. In Fig. 4, the samples can be seen positioned in an organizer box made by 3D printing.

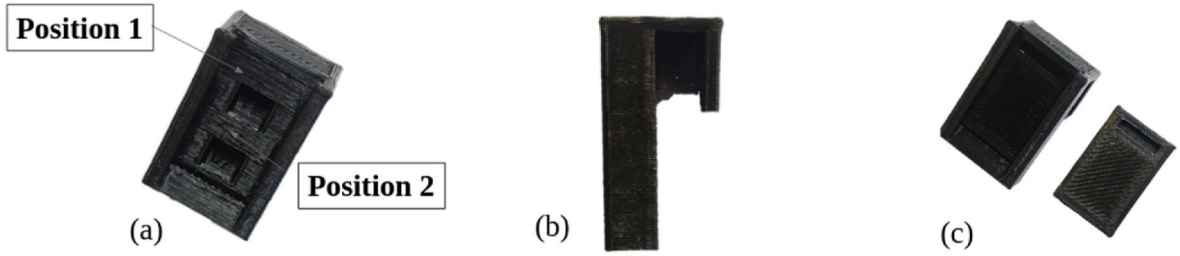

Fig. 3. Views of the dosimeter holder: (a) Upper view, (b) Side view and (c) Dosimeter holder + sup-on lid.

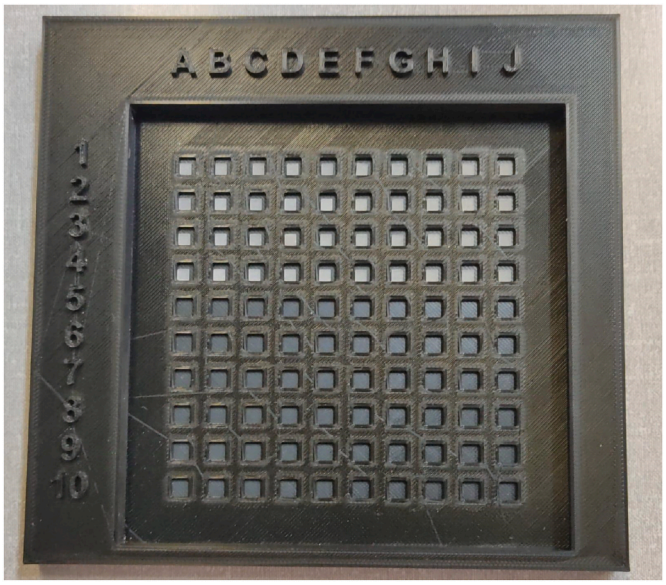

Fig. 4. 3D-printed organizational box for storing LiF:Mg,Ti detectors.

2.3. Irradiation system parameters

The irradiations were conducted using Pantak/Seifert X-ray equipment, model Isovolt 60 HS (Fig. 5). The exposures were performed with a dose of 10 mSv, 80 kV voltage and 65.2 keV energy. The energy of 60 ± 5 keV is recommended by ISO 12794. The energy range commonly used in interventional radiology can vary between 24 and 100 keV (ICRU, 2017).

The distance from the source to the object was 2.5 m, using quality N-100. Table 2 shows, in summary, the qualities recommended by ISO (ISO, 2019), implemented in the Pantak/Seifert System used in this work.

2.4. Evaluation of angular dependence

The dosimeters were divided into 6 groups, with 5 dosimeters each. Irradiation was performed with a conventional dose of 10 mSv, and the dosimeters were positioned on the sides of the phantoms, at 0° and 90° in relation to the radiation beam. The groups were positioned as follows:

Anthrop. - A: anterior region of the anthropomorphic phantom (0°);

Anthrop. - L: 90° to the left region of the anthropomorphic phantom;

Anthrop. - R: 90° to the right region of the anthropomorphic phantom;

Cylinder - A: anterior region of the cylinder recommended by ICRU (0°);

Cylinder - L: 90° to the left region of the cylinder phantom;

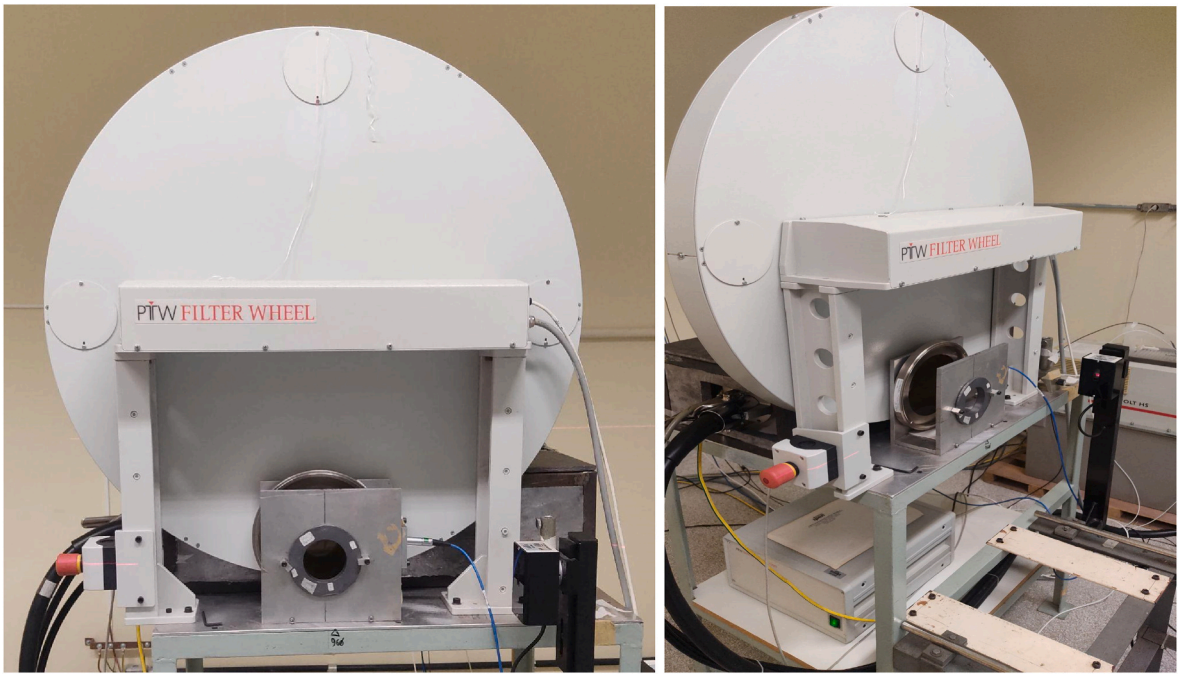

Fig. 5. X-ray equipment.

Table 2
Characteristics of narrow spectrum series (N series), adapted from ISO 4037-1-2019.

Radiation quality	Tube potential (kV)	$\bar{E}$ (Φ) keV	Recommended inherent filtration	Additional filtration, thickness, *D*, in			
				mm Pb	mm Sn	mm Cu	mm Al
N-30	30	24.6	1 mm Be				4.0
N-40	40	33.3	4 mm Al			0.21	
N-60	60	47.9	4 mm Al			0.6	
N-80	80	65.2	4 mm Al			2.0	
N-100	100	83.3	4 mm Al			5.0	
N-120	120	100	4 mm Al		1.0	5.0	
N-150	150	118	4 mm Al		2.5		

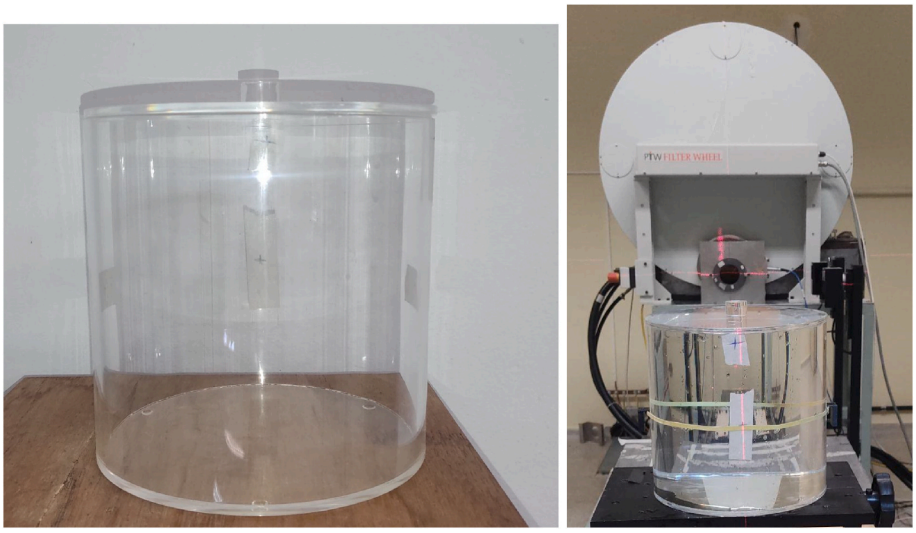

Fig. 6. (a) Phantom recommended by ICRU, (b) Arrangement for irradiation in the standard ICRU phantom.

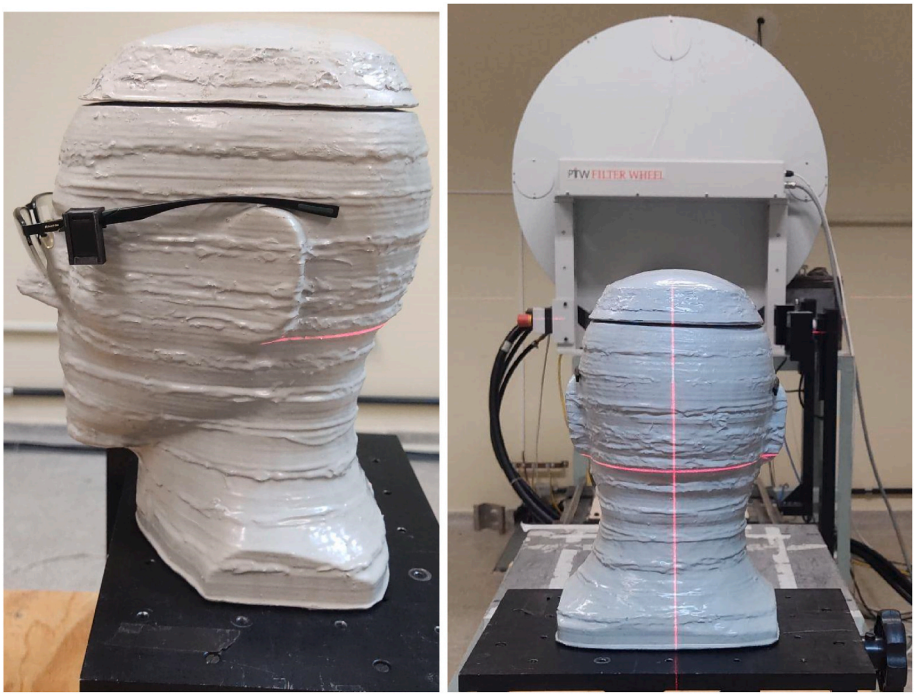

Fig. 7. (a) Phantom anthropomorphic, (b) Arrangement for irradiation in the anthropomorphic phantom.

Table 3
Characteristics of the phantoms used.

Characteristics	ICRU	Anthropomorphic
Distance between the dosimeter holder positioned on the right and left	20 cm	15.5 cm
Distance to the frontal region of the phantom	8.5 cm	5 cm
Height at which the dosimeter holder was positioned on the phantom	9.5 cm	18 cm
Weight	6.5 kg[a]	5.25 kg

[a] Filled with water.

Cylinder - R: 90° to the right region of the cylinder phantom.

To calculate angular dependence, it is necessary to define the average of the evaluated values ($\bar{E}_i$) and their respective standard deviations (s_i). The final result cannot exceed the lower limit of 0.85 and the upper limit of 1.15, as shown in Equation (1).

$$0.85 \geq \frac{\sum \bar{E}_i}{4\bar{E}_1} \pm I \leq 1.15 \quad \text{Equation (1)}$$

To find the value of I, which is the half-width of the confidence interval of x, we must first define the value of I_i, which is the width of the confidence interval (Equation (2)).

$$I_i = \frac{t_n\, s_i}{\sqrt{n_i}} \quad \text{Equation (2)}$$

where, s_i is the standard deviation, t_n is the t-student for the sample population and n_i is the number of samples. The value of t_n for 05 samples is 2.78.

The limits of variation must be stated for a quantity x, the average value is given by Equation (3):

$$\bar{x} = f(\bar{x}_1, \bar{x}_2, \bar{x}_3 \ldots \bar{x}_k) \quad \text{Equation (3)}$$

Na equação 4 é definido o valor de *I*:

$$\bar{x} = \bar{x}_1 \pm \bar{x}_2 \text{ hence } I = \sqrt{I_1^2 + I_2^2} \quad \text{Equation (4)}$$

2.5. Phantoms

The ICRU recommended phantom (Fig. 6) is described in ICRU Report 57, published in 1998, entitled "Radiation Dosimetry for Radiotherapy and Related Fields: Phantom for Radiation Dosimetry for Radiotherapy". This phantom is a cylinder-shaped phantom made of polymethylmethacrylate (PMMA) and has a space for filling with water.

The anthropomorphic phantom (Fig. 7) is entirely 3D printed, reproducing the head and neck region, developed for research purposes and studies in diagnostic imaging.

The characteristics of these phantoms can be observed in Table 3.

3. Results and discussions

Overall, it is possible to observe a relationship between the doses received by the two phantoms, with the dosimeters positioned in the anterior region presenting the highest averages.

The dosimeters used in the Cylinder presented a higher average when comparing the same positions of the anthropomorphic phantom. This may be associated with the fact that the cylinder has a larger circumference.

These results can be seen in Table 4.

The results obtained using the equations recommended by ISO 12794 were within the limits established by the equation (Table 5). Fig. 8 shows the distribution of the results after applying Equation (1).

4. Conclusions

The results presented in this work attest to the effectiveness of the dosimeter holders developed using 3D printing in meeting the specifications of ISO 12794.

It is also possible to state that, for this test, there was no significant difference between the phantoms, and a relatively higher dose received in the cylinder filled with water could be observed.

Therefore, the dosimeter holder developed was approved in the adapted angular dependence test, and can be used on the temple of glasses or in conjunction with a band in the forehead region.

CRediT authorship contribution statement

G.G. Nascimento: Writing – original draft, Visualization, Project administration, Methodology, Investigation, Formal analysis, Data curation. **O. Rodrigues:** Writing – review & editing, Supervision. **M. Savi:** Writing – review & editing. **D. Villani:** Writing – review & editing.

Table 5
Results after applying Equation 1.

Phantoms	$\bar{E}_i$	I	Equation 1	Results
Anthrop. - A	10.373	0.0136	$0.85 \geq \frac{\sum \bar{E}_i}{4\bar{E}_1} \pm I \leq 1.15$	0.986 ± 0.136
Anthrop. - L	10.307			1.017 ± 0.136
Anthrop. - R	11.878			1.024 ± 0.136
Cylinder - A	11.114			0.978 ± 0.136
Cylinder - L	10.359			1.011 ± 0.136
Cylinder - R	11.406			0.996 ± 0.136

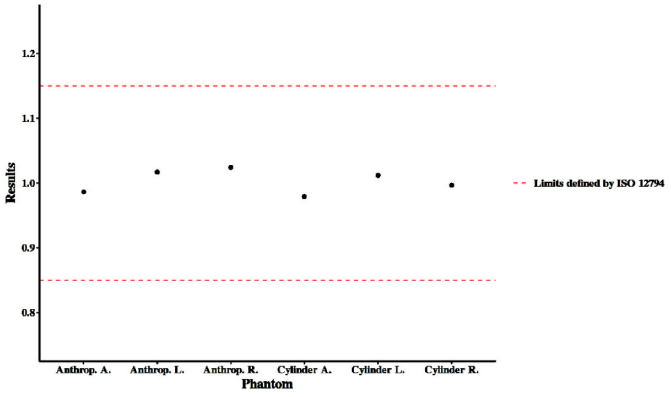

Fig. 8. Results obtained after applying Equation (1).

Table 4
Results of irradiations in the standard ICRU phantom and anthropomorphic phantom.

Phantom	Response (mSv)					Mean (mSv)	Standard deviation (%)
Anthrop. - A	11.12	10.57	10.21	10.60	10.62	10.62	0.32
Anthrop. - L	10.55	9.72	9.26	9.88	12.10	10.30	1.10
Anthrop. - R	11.87	9.97	9.25	9.84	10.91	10.37	1.03
Cylinder - A	11.11	10.78	9.99	10.21	11.44	10.71	0.61
Cylinder - L	10.42	9.28	10.12	10.75	11.21	10.35	0.73
Cylinder - R	11.40	9.15	9.49	11.39	11.14	10.51	1.37

M.P.A. Potiens: Writing – review & editing, Supervision.

Declaration of competing interest

The authors of this work state that this study has no conflicts of interest.

Acknowledgments

The authors of this work would like to thank CNPq (process 140973/2023-0) and FAPESP (process 2017/50332-0) for the support granted.

Data availability

Data will be made available on request.

References

Alyahyawi, A., Dimitriadis, A., Jafari, S.M., Lohstroh, A., Alanazi, A., Alsubaie, A., Clark, C.H., Nisbet, A., Bradley, D.A., 2019. Thermoluminescence measurements of eye-lens dose in a multi-centre stereotactic radiosurgery audit. Radiat. Phys. Chem. 155, 75–81. https://doi.org/10.1016/j.radphyschem.2018.08.030.

Barbosa, A.H.P., Medeiros, R.B., Corpa, A.M.R., Higa, F.S., Souza, M.T.D., Barbosa, P.L., Moreira, A.C., Quadros, A.S.D., Lemke, V.D.M.G., Cantarelli, M.J.D.C., 2019. Prevalence of lens opacity in interventional cardiologists and professional working in the hemodynamics in Brazil. Arq. Bras. Cardiol. https://doi.org/10.5935/abc.20190028.

Behrens, R., 2011. Monitoring the eye lens. Acta Ophthalmol. 89 (s248). https://doi.org/10.1111/j.1755-3768.2011.2163.x, 0–0.

Bitarafan Rajabi, A., Noohi, F., Hashemi, H., Haghjoo, M., Miraftab, M., Yaghoobi, N., Rastgou, F., Malek, H., Faghihi, H., Firouzabadi, H., Asgari, S., Rezvan, F., Khosravi, H., Soroush, S., Khabazkhoob, M., 2015. Ionizing radiation-induced cataract in interventional cardiology staff. Res. Cardiovasc. Med. 4 (1), e25148. https://doi.org/10.5812/cardiovascmed.25148.

International Commission on Radiological Protection, 2012. ICRP Publication 118: ICRP statement on tissue reactions and early and late effects of radiation in normal tissues and organs - threshold doses for tissue reactions in a radiation protection context. Ann. ICRP 41 (1–2), 1–322. https://doi.org/10.1016/j.icrp.2012.02.001.

International Commission on Radiological Protection, 2007. ICRP publication 103: the 2007 recommendations of the international commission on radiological protection. Ann. ICRP 37 (2–4), 1–332.

International Commission on Radiological Protection, 1991. ICRP publication 60: 1990 recommendations of the international commission on radiological protection. Ann. ICRP 21 (1–3), 1–201.

International Commission on Radiation Units and Measurements, 1985. ICRU Report 57: Radiation Dosimetry: Electron Beams with Energies between 1 and 50 MeV. ICRU, Bethesda, MD.

International Commission on Radiation Units and Measurements, 2017. ICRU Report 95: operational quantities for external radiation exposure. J. ICRU 15 (1), 1–74.

International Organization for Standardization, 2019. ISO 4037-1:2019: X and gamma reference radiation for calibrating dosemeters and doserate meters and for determining their response as a function of photon energy - Part 1. Radiat. Charact. Prod. Method.

International Organization for Standardization, 2014. ISO 12794:2000: Nuclear Energy - Radiation Protection - Individual Thermoluminescence Dosemeters for Extremities and Eyes.

Petoussi-Henss, N., Satoh, D., Endo, A., Eckerman, K.F., Bolch, W.E., Hunt, J., Jansen, J. T.M., Kim, C.H., Lee, C., Saito, K., Schlattl, H., Yeom, Y.S., Yoo, S.J., 2020. ICRP publication 144: dose coefficients for external exposures to environmental sources. Ann. ICRP 49 (2), 11–145. https://doi.org/10.1177/0146645320906277.

Savi, M.B.M.B., 2022. Estudo de materiais e desenvolvimento de um simulador antropomórfico de cabeça e pescoço por meio de impressão 3D [Tese de Doutorado em Tecnologia Nuclear - Aplicações. Universidade de São Paulo. https://doi.org/10.11606/T.85.2022.tde-04082022-143618.

Surić Mihić, M., Pavelić, L., Vojnić Kortmiš, M., Šiško, J., Maltar-Strmečki, N., Prlić, I., 2020. 3D-printed eye lens dosemeter holder for use in interventional radiology and interventional cardiology. Radiat. Meas. 135, 106385. https://doi.org/10.1016/j.radmeas.2020.106385.